A unified framework for forward and inverse modeling of ice sheet flow using physics-informed neural networks

Gong Cheng[1], Mathieu Morlighem[1], and Sade Francis[1]

[1]Dartmouth College

March 05, 2024

Abstract

Predicting the future contribution of the ice sheets to sea level rise over the next decades presents several challenges due to a poor understanding of critical boundary conditions, such as basal sliding. Traditional numerical models often rely on data assimilation methods to infer spatially variable friction coefficients by solving an inverse problem, given an empirical friction law. However, these approaches are not versatile, as they sometimes demand extensive code development efforts when integrating new physics into the model. Furthermore, this approach makes it difficult to handle sparse data effectively. To tackle these challenges, we propose a novel approach utilizing Physics-Informed Neural Networks (PINNs) to seamlessly integrate observational data and governing equations of ice flow into a unified loss function, facilitating the solution of both forward and inverse problems within the same framework. We illustrate the versatility of this approach by applying the framework to two-dimensional problems on the Helheim Glacier in southeast Greenland. By systematically concealing one variable (e.g. ice speed, ice thickness, etc.), we demonstrate the ability of PINNs to accurately reconstruct hidden information. Furthermore, we extend this application to address a challenging mixed inversion problem. We show how PINNs are capable of inferring the basal friction coefficient while simultaneously filling gaps in the sparsely observed ice thickness. This unified framework offers a promising avenue to enhance the predictive capabilities of ice sheet models, reducing uncertainties, and advancing our understanding of poorly constrained physical processes.

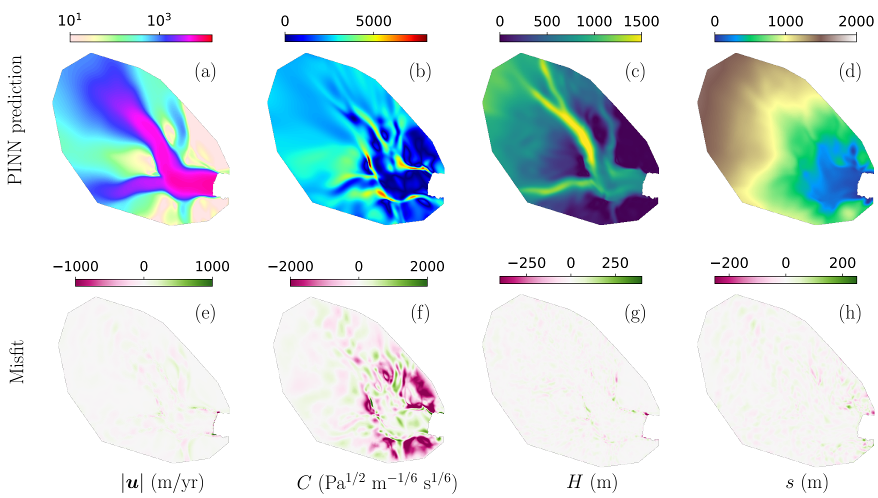

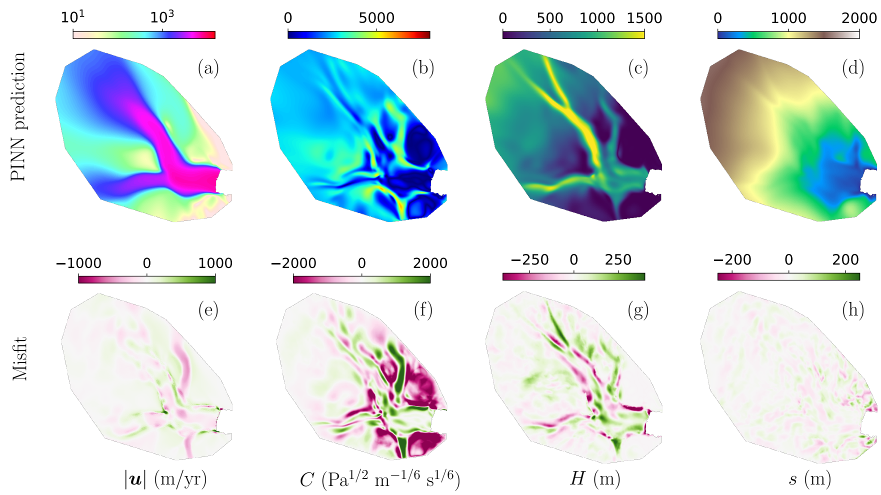
PINN prediction
Misfit
(a)
(b)
(c)
(d)
(e)
(f)
(g)
(h)
10^1
10^3
0
5000
0
500
1000
1500
0
1000
2000
−1000
0
1000
−2000
0
2000
−250
0
250
−200
0
200
$|\boldsymbol{u}|$ (m/yr)
C (Pa$^{1/2}$ m$^{-1/6}$ s$^{1/6}$)
H (m)
s (m)

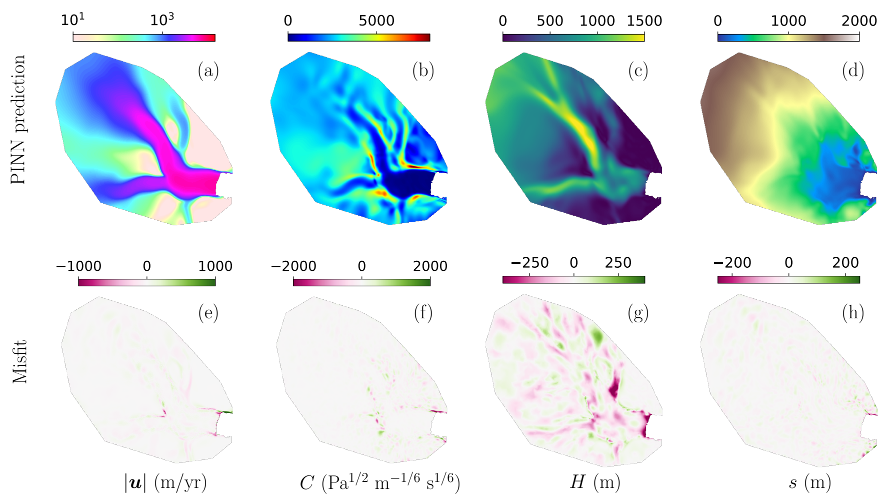
PINN prediction
Misfit
(a)
(b)
(c)
(d)
(e)
(f)
(g)
(h)
10^1
10^3
0
5000
0
500
1000
1500
0
1000
2000
−1000
0
1000
−2000
0
2000
−250
0
250
−200
0
200
$|\boldsymbol{u}|$ (m/yr)
C (Pa$^{1/2}$ m$^{-1/6}$ s$^{1/6}$)
H (m)
s (m)

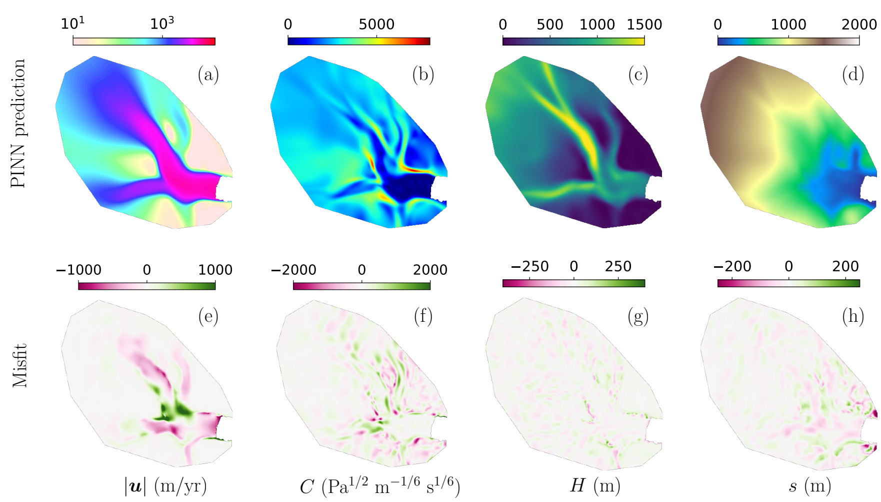
PINN prediction
Misfit
(a)
(b)
(c)
(d)
(e)
(f)
(g)
(h)
10^1
10^3
0
5000
0
500
1000
1500
0
1000
2000
−1000
0
1000
−2000
0
2000
−250
0
250
−200
0
200
$|\boldsymbol{u}|$ (m/yr)
C (Pa$^{1/2}$ m$^{-1/6}$ s$^{1/6}$)
H (m)
s (m)

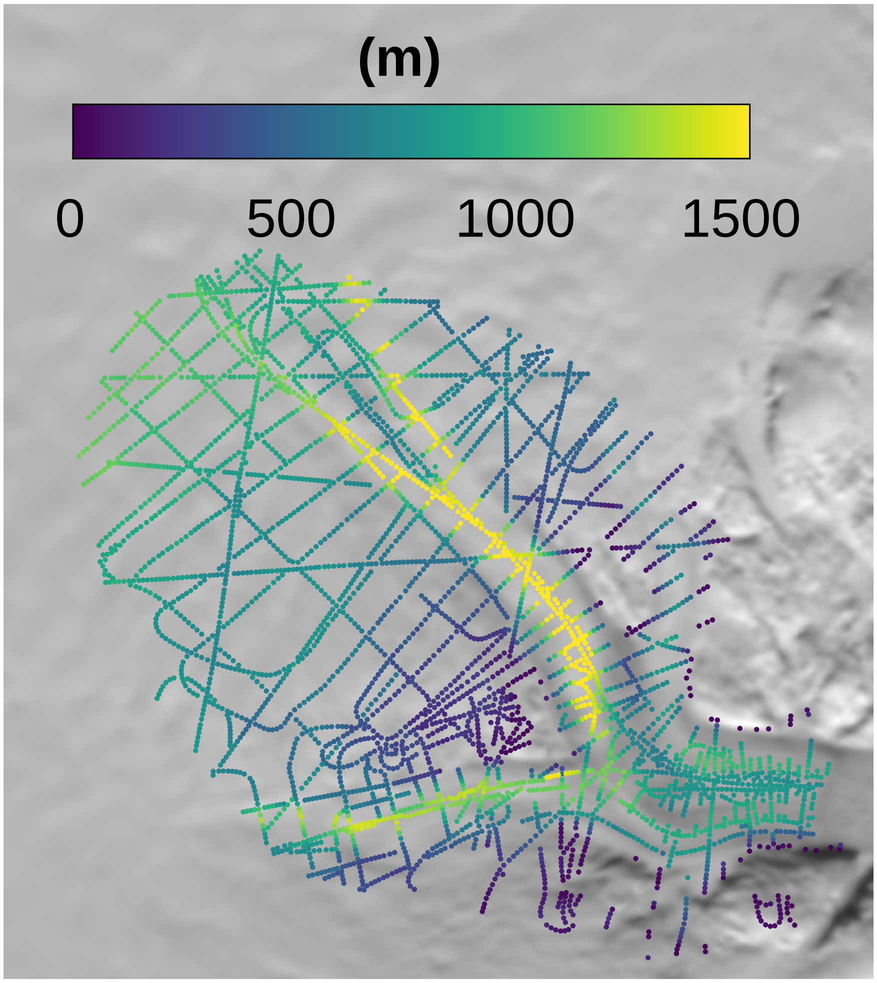
(m)
0
500
1000
1500

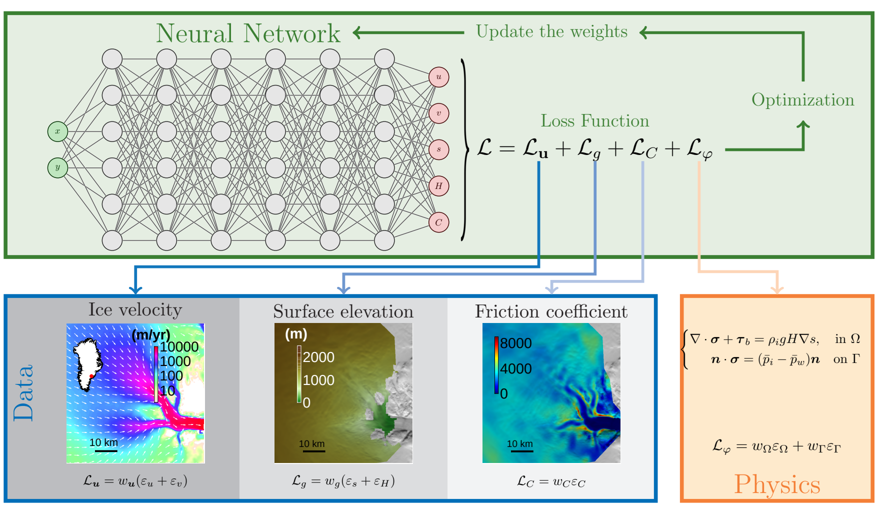
Neural Network
Update the weights
Optimization
Loss Function
$\mathcal{L} = \mathcal{L}_{\mathbf{u}} + \mathcal{L}_g + \mathcal{L}_C + \mathcal{L}_\varphi$
Data
Ice velocity
(m/yr)
10000
1000
100
10
10 km
$\mathcal{L}_{\mathbf{u}} = w_{\mathbf{u}}(\varepsilon_u + \varepsilon_v)$
Surface elevation
(m)
2000
1000
0
10 km
$\mathcal{L}_g = w_g(\varepsilon_s + \varepsilon_H)$
Friction coefficient
8000
4000
0
10 km
$\mathcal{L}_C = w_C \varepsilon_C$
$\begin{cases} \nabla \cdot \boldsymbol{\sigma} + \boldsymbol{\tau}_b = \rho_i g H \nabla s, & \text{in } \Omega \\ \boldsymbol{n} \cdot \boldsymbol{\sigma} = (\bar{p}_i - \bar{p}_w)\boldsymbol{n} & \text{on } \Gamma \end{cases}$
$\mathcal{L}_\varphi = w_\Omega \varepsilon_\Omega + w_\Gamma \varepsilon_\Gamma$
Physics

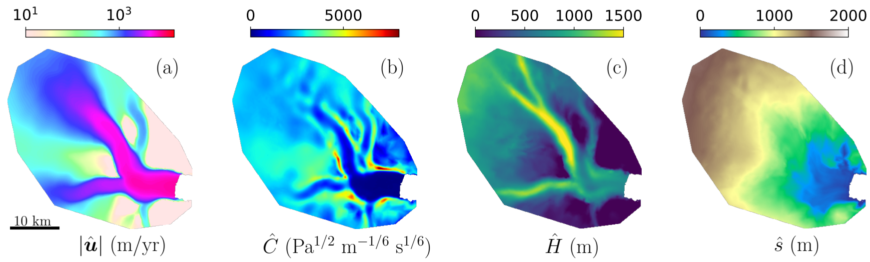
(a)
(b)
(c)
(d)
10 km
$|\hat{\boldsymbol{u}}|$ (m/yr)
$\hat{C}$ (Pa$^{1/2}$ m$^{-1/6}$ s$^{1/6}$)
$\hat{H}$ (m)
$\hat{s}$ (m)

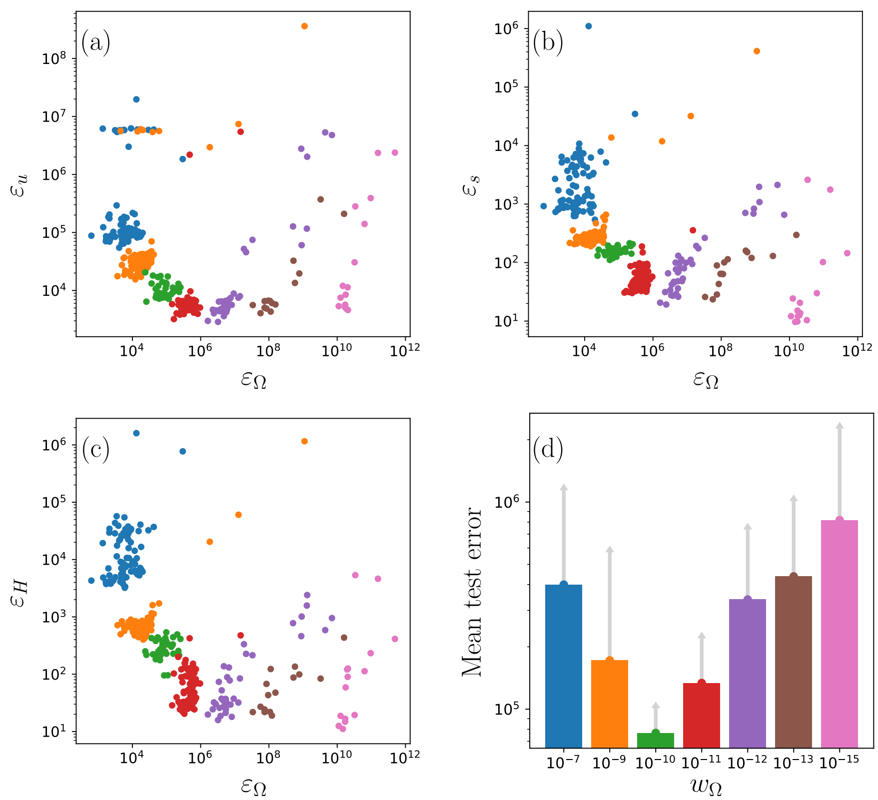
(a)
(b)
(c)
(d)
ε_u
ε_s
ε_H
ε_Ω
Mean test error
w_Ω

Figure 3. MSE of the (a) velocity, (b) surface elevation, and (c) ice thickness versus the PDE residual ϵ. (d) The mean test error of the PINNs predictions using different weights w.

193.75 m/yr. This represents approximately less than 10% of the average flow velocity over the entire domain (2,028.69 m/yr) and about 2.7% of the highest velocity (7,152.93 m/yr).

3.3 Inverse problem

We change the training dataset to use ice velocity $\hat{u}$, ice thickness $\hat{H}$, and surface elevation $\hat{s}$. In this configuration, the PINN serves as an inverse solver to infer the basal friction coefficient C. Again, because we don't expose the PINN to the "true" friction coefficient from the ISSM model inversion, the PINN is inferring C solely based on the PDE constraint that is linking the friction coefficient to the other variables that the PINN is exposed to. The predictions and misfits are presented in Figure 5, and the RMSE of the misfit is provided in Table 2. Similar to the forward problem in section 3.2, the predictions of PINN align well with the "true" solution. Particularly for those learning from the reference data, the relative errors are all below 3% (the average ice thickness is 761.16 m, and the average surface elevation is 986.76 m).

The RMSE of the misfit in C is 589.61 $\mathrm{Pa}^{1/2}\,\mathrm{m}^{-1/6}\,\mathrm{s}^{1/6}$. However, as shown in Figure 5(f), the pattern of large errors is located primarily in the slow-moving region (veillustrates all available flight tracks around Helheim Glacier, with dots representing resampled points at 200 m intervals along the tracks. These flight track data are notably sparse, even along the main branch of Helheim Glacier, where only one flight track is present in the center of the ice stream. Various numerical methods have been developed to leverage flight track data along with other observations to fill gaps in regions lacking direct measurements. Some examples include the BedMachine Greenland and Antarctica models (Morlighem et al., 2017, 2020), which use mass conservation principles to constrain ice thickness.

Figure 7. Available ice thickness data in the region of interest. The dots are resampled at 200 m intervals, overlaid with an image map from MEaSUREs MODIS Mosaic of Greenland (Haran et al., 2018).

Given the flexibility of the PINN, we perform one more test here to assess its ability to address a *dual* inversion problem. Here we would like to test the ability of the PINN to infer the basal friction coefficient, C, while simultaneously filling gaps in sparsely observed ice thickness, H. Following the same procedure as the ones described above, we expose the model to ice velocity, $\hat{u}$, surface elevation, $\hat{s}$, and ice thickness only along flight tracks, H, as shown in Figure 7. The predictions from the PINN and their corresponding misfits are presented in Figure 8. Notably, the PINN predictions for ice velocity and surface elevation align well with the true solutions (shown in Figure 2), and the RMSE of the misfits are 126.83 m/yr for the velocity and 22.08 m for the surface elevation. Both are below those obtained in the forward problem (193.75 m/yr and 26.99 m). The predicted ice thickness closely reproduces the shape and magnitude observed in the true solution as well. While the predicted friction coefficient shows a high misfit in slow-moving regions, as expected given the limitations of SSA in slow-moving regions discussed above, it aligns well with the true solution in fast-flow regions. The RMSE values for both C and H are comparable to those obtained in the individual inversions discussed in sections 3.3 and 3.4 (see Table 2).

It is important to note that only the ice velocity, surface elevation, and ice thickness along flight lines are incorporated into the training procedure and exposed to the PINN. The governing equation in the PINN is based on momentum conservation rather than mass conservation, which is the principle employed by BedMachine for inferring ice thickness. Consequently, discrepancies between the PINN predictions and the reference ice thickness from BedMachine are expected, constituting the likely primary reason for the observed misfit in Figure 8 (g). Furthermore, considering that the reference friction coefficient is inferred from ISSM using the ice thickness from BedMachine, differences are expected, particularly in regions where the two ice thickness datasets diverge.

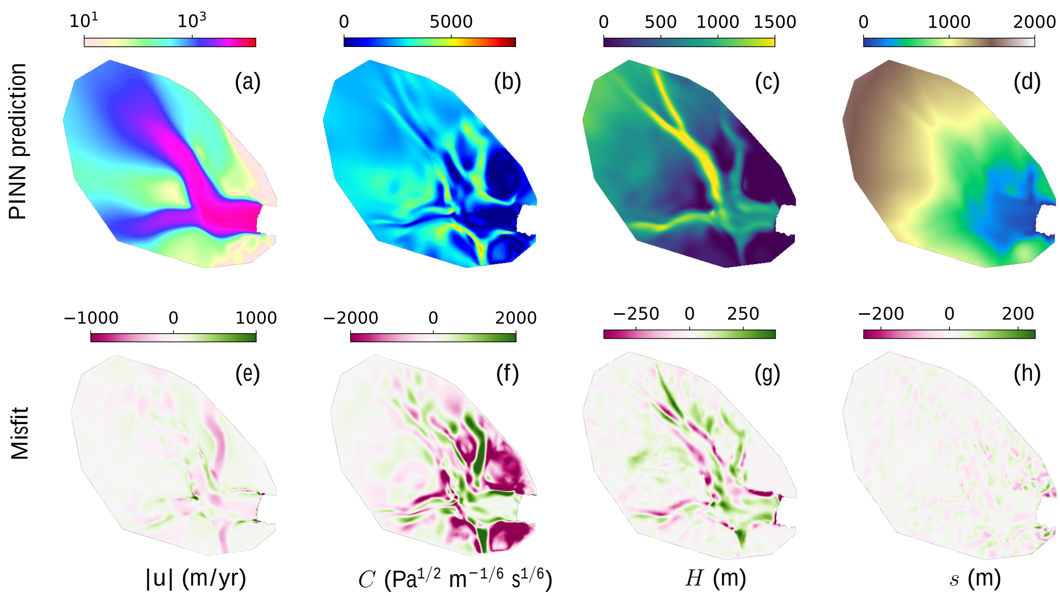

Figure 8. (a)-(d) Predictions of the PINN inferring ice thickness and basal friction coefficient using ice velocity $\hat{\boldsymbol{u}}$, surface elevation $\hat{s}$, and flight track data $\bar{H}$ (as in Figure 7) in the training procedure. (e)-(h) Corresponding misfits between the predictions and their corresponding reference data in Figure 2.

4.4 Limitations

While our study highlights the capabilities of PINNs in ice sheet modeling, certain limitations should be acknowledged. For the forward model, which is mathematically well-posed, traditional grid-based solvers clearly outperform PINNs (Karniadakis et al., 2021). For instance, while training the PINN for a forward problem (section 3.2) requires approximately 10 hours on one GPU, the same problem can be solved within minutes using established solvers like ISSM with 40 CPUs for a mesh of approximately 2,000 elements. Another challenge is that the governing equations are imposed as soft constraints in the loss function and compete with the data misfit during the optimization, causing occasional non-convergence. Furthermore, it is well known that SSA serves as a reliable approximation for ice dynamics in fast-flowing regions but its assumptions break down in the interior of the ice sheet. Generalizing this approach to the entire Greenland Ice Sheet may necessitate the use of alternative physics or a combination of different physics to infer ice thickness, for example.

Future research directions will need to address the identified limitations and further enhance the application of PINNs in ice sheet modeling. To enhance its efficiency, the training process could be optimized and potentially integrate parallel computing strategies for faster execution. The handling of PDEs as soft constraints in the PINN framework could be revised in order to mitigate convergence issues. Finally, improving the accuracy of the ice sheet interior will involve alternative physics or hybrid approaches that better capture the complexities of ice dynamics in slow-moving regions. These steps will collectively contribute to advancing the robustness, accuracy, and computational efficiency of PINNs for comprehensive ice sheet modeling.

5 Conclusion

This study explores several applications of PINNs in typical problems of ice sheet modeling. In contrast to traditional numerical methods, we utilize PINNs to construct a unified framework for both forward and inverse modeling. The inherent adaptability of PINNs is particularly easy to use and expand, enabling the inclusion of new physical parameters into the numerical model. This approach offers a promising avenue for enhancing the flexibility of ice sheet models and data assimilation, beyond the traditional categories of forward or inverse problems.

The dual inversion case presented in this study further demonstrates the ability of PINNs to simultaneously infer the basal friction coefficient and fill in gaps in partially sparse ice thickness observations. PINNs, with their capacity to integrate data misfit and physical principles, contribute to advancing numerical ice sheet modeling. This study suggests the potential of PINNs in improving our understanding of ice dynamics, contributing to more accurate predictions of future sea-level rise in glaciology and climate science.

6 Open Research

The data and the code of the simulations are available at `https://doi.org/10.5281/zenodo.10627691`. ISSM (Larour et al., 2009) is open source and available at `https://doi.org/10.5281/zenodo.7850841`.

Acknowledgments

This work was supported by the Heising Simons Foundation grant 2019-1161 and 2021-3059, and the National Science Foundation #2118285.

References

Akesson, H., Morlighem, M., O'Regan, M., & Jakobsson, M. (2021). Future Projections of Petermann Glacier Under Ocean Warming Depend Strongly on Friction Law. *J. Geophys. Res. - Earth Surface*, *126*(6), e2020JF005921. Retrieved from `https://agupubs.onlinelibrary.wiley.com/doi/abs/10.1029/2020JF005921` doi: 10.1029/2020JF005921

Barnes, J. M., dos Santos, T. D., Goldberg, D., Gudmundsson, G. H., Morlighem, M., & De Rydt, J. (2021). The transferability of adjoint inversion products between different ice flow models. *Cryosphere*, *15*(4), 1975–2000. Retrieved from `https://tc.copernicus.org/articles/15/1975/2021/` doi: 10.5194/tc-15-1975-2021

Brondex, J., Gagliardini, O., Gillet-Chaulet, F., & Durand, G. (2017). Sensitivity of grounding line dynamics to the choice of the friction law. *J. Glaciol.*, *63*(241), 854-866. doi: 10.1017/jog.2017.51

Brondex, J., Gillet-Chaulet, F., & Gagliardini, O. (2019). Sensitivity of centennial mass loss projections of the Amundsen basin to the friction law. *Cryosphere*, *13*, 177-195. doi: 10.5194/tc-13-177-2019

Budd, W. F., Keage, P. L., & Blundy, N. A. (1979). Empirical studies of ice sliding.

J. Glaciol., *23*, 157-170.

Bueler, E., & Brown, J. (2009, JUL 31). Shallow shelf approximation as a \sliding law" in a thermomechanically coupled ice sheet model. *J. Geophys. Res.*, *114*, 1-21. doi: 10.1029/2008JF001179

Cheng, G., & Lotstedt, P. (2020, FEB 17). Parameter sensitivity analysis of dynamic ice sheet models - numerical computations. *CRYOSPHERE*, *14*(2), 673-691. doi: 10.5194/tc-14-673-2020

Colinge, J., & Blatter, H. (1998). Stress and velocity elds in glaciers: Part I. Finite-di erence schemes for higher-order glacier models. *J. Glaciol.*, *44*(148), 448-456.

Cu ey, K. M., & Paterson, W. S. B. (2010). *The Physics of Glaciers, 4th Edition* (Butterworth-Heinemann, Ed.). Elsevier, Oxford.

Durand, G., Gagliardini, O., Zwinger, T., Le Meur, E., & Hindmarsh, R. C. A. (2009). Full Stokes modeling of marine ice sheets: in uence of the grid size. *Ann. Glaciol.*, *50*(52), 109-114.

Eyring, V., Bony, S., Meehl, G. A., Senior, C. A., Stevens, B., Stou er, R. J., & Taylor, K. E. (2016). Overview of the Coupled Model Intercomparison Project Phase 6 (CMIP6) experimental design and organization. *Geosci. Model Dev.*, *9*(5), 1937{1958. Retrieved from `http://www.geosci-model-dev.net/9/1937/2016/` doi: 10.5194/gmd-9-1937-2016

Frederikse, T., Landerer, F., Caron, L., Adhikari, S., Parkes, D., Humphrey, V. W., ... Wu, Y.-H. (2020, Aug 01). The causes of sea-level rise since 1900. *Nature*, *584*(7821), 393-397. Retrieved from `https://doi.org/10.1038/s41586-020-2591-3` doi: 10.1038/s41586-020-2591-3

Gagliardini, O., Cohen, D., Raback, P., & Zwinger, T. (2007, MAY 31). Finite-element modeling of subglacial cavities and related friction law. *J. Geophys. Res. - Earth Surface*, *112*(F2), 1-11. doi: 10.1029/2006JF000576

Glen, J. W. (1958). The ow law of ice: A discussion of the assumptions made in glacier theory, their experimental foundations and consequences. *IASH Publ*, *47*, 171{183.

Goldberg, D. N., & Sergienko, O. V. (2011). Data assimilation using a hybrid ice ow model. *Cryosphere*, *5*(2), 315-327. doi: 10.5194/tc-5-315-2011

Griewank, A., Juedes, D., & Utke, J. (1996). ADOL-C: A Package for the Automatic Di erentiation of Algorithms Written in C/C++. *ACM Trans. Math. Software*, *22*(2), 131{167. Retrieved from `http://doi.acm.org/10.1145/229473.229474`

Haran, T., Bohlander, J., Scambos, T., Painter, T., & Fahnestock, M. (2018). *MEaSUREs MODIS Mosaic of Greenland (MOG) 2005, 2010, and 2015 Image Maps, Version 2.* Boulder, Colorado USA. NASA National Snow and Ice Data Center Distributed Active Archive Center. Retrieved from `https://doi.org/10.5067/9ZO79PHOTYE5` doi: 10.5067/9ZO79PHOTYE5

Howat, I. M., Negrete, A., & Smith, B. E. (2014). The Greenland Ice Mapping Project (GIMP) land classi cation and surface elevation datasets. *Cryosphere*, *8*(4), 1509-1518. Retrieved from `http://www.the-cryosphere.net/8/1509/2014/tc-8-1509-2014.html` doi: 10.5194/tc-8-1509-2014

Iwasaki, Y., & Lai, C.-Y. (2023, NOV 1). One-dimensional ice shelf hardness inversion: Clustering behavior and collocation resampling in physics-informed neural networks. *J. Comput. Phys.*, *492*. doi: 10.1016/j.jcp.2023.112435

Joughin, I., Smith, B. E., & Howat, I. M. (2018, February). A complete map of Greenland ice velocity derived from satellite data collected over 20 years. *J. Glaciol.*, *64*(243), 1-11. doi: 10.1017/jog.2017.73

Karniadakis, G. E., Kevrekidis, I. G., Lu, L., Perdikaris, P., Wang, S., & Yang, L. (2021, JUN). Physics-informed machine learning. *Nat. Rev. Phys.*, *3*(6), 422-440. doi: 10.1038/s42254-021-00314-5

Larour, E., Rignot, E., Seroussi, H., Morlighem, M., & Schiermeier, J. (2009). *ISSM* *website.* (http://issm.jpl.nasa.gov)

Larour, E., Seroussi, H., Morlighem, M., & Rignot, E. (2012, Mar). Continental scale, high order, high spatial resolution, ice sheet modeling using the Ice Sheet System Model (ISSM). *J. Geophys. Res.*, *117*(F01022), 1-20. doi: 10.1029/2011JF002140

Lu, L., Meng, X., Mao, Z., & Karniadakis, G. E. (2021, MAR). DeepXDE: A Deep Learning library for solving di erential equations. *SIAM Rev.*, *63*(1), 208-228. doi: 10.1137/19M1274067

MacAyeal. (1989, APR 10). Large-scale ice ow over a viscous basal sediment: Theory and application to Ice Stream B, Antarctica. *J. Geophys. Res.*, *94*(B4), 4071-4087.

MacAyeal, D. (2002, DEC). *Notes on ice stream inverse code finite element solution for ice stream equations.* (copy of a document printed in 2002)

Mangeney, A., & Califano, F. (1998, JAN 10). The shallow ice approximation for anisotropic ice: Formulation and limits. *J. Geophys. Res.*, *103*(B1), 691-705.

Morlighem, M., & Goldberg, D. (2023, June). Data Assimilation in Glaciology. In A. Ismail-Zadeh, F. Castelli, D. Jones, & S. Sanchez (Eds.),*Applications of data assimilation and inverse problems in the earth sciences.* Cambridge University Press.

Morlighem, M., Rignot, E., Binder, T., Blankenship, D., Drews, R., Eagles, G., . . . Young, D. A. (2020). Deep glacial troughs and stabilizing ridges unveiled beneath the margins of the Antarctic ice sheet. *Nat. Geosci.*, *13*(2), 132{137. doi: 10.1038/s41561-019-0510-8

Morlighem, M., Rignot, E., Seroussi, H., Larour, E., Ben Dhia, H., & Aubry, D. (2010, JUL). Spatial patterns of basal drag inferred using control methods from a full-Stokes and simpler models for Pine Island Glacier, West Antarctica. *Geophys. Res. Lett.*, *37*(L14502), 1-6. doi: 10.1029/2010GL043853

Morlighem, M., Seroussi, H., Larour, E., & Rignot, E. (2013, SEP). Inversion of basal friction in Antarctica using exact and incomplete adjoints of a higher-order model. *J. Geophys. Res.*, *118*(3), 1746-1753. doi: 10.1002/jgrf.20125

Morlighem, M., Williams, C. N., Rignot, E., An, L., Arndt, J. E., Bamber, J. L., . . . Zinglersen, K. B. (2017). BedMachine v3: Complete bed topography and ocean bathymetry mapping of Greenland from multi-beam echo sounding combined with mass conservation. *Geophys. Res. Lett.*, *44*(21), 11,051{11,061. Retrieved from `http://dx.doi.org/10.1002/2017GL074954` (2017GL074954) doi: 10.1002/2017GL074954

Mouginot, J., Rignot, E., Bj rk, A. A., van den Broeke, M., Millan, R., Morlighem, M., . . . Wood, M. (2019). Forty-six years of greenland ice sheet mass balance from 1972 to 2018. *Proc. Natl. Acad. Sci.*. Retrieved from `https://www.pnas.org/content/early/2019/04/16/1904242116` doi: 10.1073/pnas.1904242116

Nowicki, S. M. J., Payne, A. J., Larour, E., Seroussi, H., Goelzer, H., Lipscomb, W. H., . . . Shepherd, A. (2016, Dec). Ice Sheet Model Intercomparison Project (ISMIP6) contribution to CMIP6 . *Geosci. Model Dev.*, *9*, 4521-4545. doi: 10.5194/gmd-9-4521-2016

Petra, N., Zhu, H., Stadler, G., Hughes, T. J. R., & Ghattas, O. (2012). An inexact Gauss-Newton method for inversion of basal sliding and rheology parameters in a nonlinear Stokes ice sheet model. *J. Glaciol.*, *58*(211), 889-903. doi: 10.3189/2012JoG11J182

Raissi, M., Perdikaris, P., & Karniadakis, G. E. (2019, FEB 1). Physics-informed neural networks: A deep learning framework for solving forward and inverse problems involving nonlinear partial di erential equations. *J. Comput. Phys.*, *378*, 686-707. doi: 10.1016/j.jcp.2018.10.045

Riel, B., Minchew, B., & Bischo , T. (2021, NOV). Data-driven inference of the sechanics of slip slong glacier beds using physics-informed neural networks: case study on Rutford Ice Stream, Antarctica. *J. Adv. Model. Earth Syst.*, *13*(11). doi: 10.1029/2021MS002621

Rignot, E., Mouginot, J., Scheuchl, B., van den Broeke, M., van Wessem, M. J., & Morlighem, M. (2019). Four decades of Antarctic Ice Sheet mass balance from 1979{2017. *Proc. Natl. Acad. Sci.*, *116*(4), 1095{1103. Retrieved from `https://www.pnas.org/content/early/2019/01/08/1812883116` doi: 10.1073/pnas.1812883116

Tarantola, A. (2005). *Inverse Problem Theory* (SIAM, Ed.). SIAM.

Vogel, C. R. (2002). *Computational Methods for Inverse Problems*. Philadelphia, PA, USA: Society for Industrial and Applied Mathematics.

Weertman, J. (1957, March). On the sliding of glaciers. *J. Glaciol.*, *3*, 33-38.

Yu, H., Rignot, E., Seroussi, H., & Morlighem, M. (2018). Retreat of Thwaites Glacier, West Antarctica, over the next 100 years using various ice ow models, ice shelf melt scenarios and basal friction laws. *Cryosphere*, *12*(12), 3861{3876. Retrieved from `https://www.the-cryosphere.net/12/3861/2018/` doi: 10.5194/tc-12-3861-2018